Journal of Hazardous Materials 211–212 (2012) 126–130

Contents lists available at SciVerse ScienceDirect

Journal of Hazardous Materials

journal homepage: www.elsevier.com/locate/jhazmat

Treatment of chemical warfare agents by zero-valent iron nanoparticles and ferrate(VI)/(III) composite

Radek Zboril[a,*], Marek Andrle[b], Frantisek Oplustil[b], Libor Machala[a], Jiri Tucek[a], Jan Filip[a], Zdenek Marusak[a], Virender K. Sharma[c,d,**]

[a] Regional Centre of Advanced Technologies and Materials, Departments of Physical Chemistry and Experimental Physics, 17. listopadu 1192/12, 771 46 Olomouc, Czech Republic
[b] Military Institute VOP-026 Sternberk, Division in Brno, Rybkova 8, 602 00 Brno, Czech Republic
[c] Chemistry Department, Florida Institute of Technology, 150 West University Boulevard, Melbourne, FL 32901, USA
[d] Center of Ferrate Excellence, Florida Institute of Technology, 150 West University Boulevard, Melbourne, FL 32901, USA

ARTICLE INFO

Article history:
Received 14 June 2011
Received in revised form 28 October 2011
Accepted 28 October 2011
Available online 7 November 2011

Keywords:
Nanoparticles
Oxidation
In situ technology
Yperite
Poison gas

ABSTRACT

Nanoscale zero-valent iron (nZVI) particles and a composite containing a mixture of ferrate(VI) and ferrate(III) were prepared by thermal procedures. The phase compositions, valence states of iron, and particle sizes of iron-bearing compounds were determined by combination of X-ray powder diffraction, Mössbauer spectroscopy and scanning electron microscopy. The applicability of these environmentally friendly iron based materials in treatment of chemical warfare agents (CWAs) has been tested with three representative compounds, sulfur mustard (bis(2-chlorethyl) sulfide, HD), soman ((3,3′-imethylbutan-2-yl)-methylphosphonofluoridate, GD), and *O*-ethyl *S*-[2-(diisopropylamino)ethyl] methylphosphonothiolate (VX). Zero-valent iron, even in the nanodimensional state, had a sluggish reactivity with CWAs, which was also observed in low degrees of CWAs degradation. On the contrary, ferrate(VI)/(III) composite exhibited a high reactivity and complete degradations of CWAs were accomplished. Under the studied conditions, the estimated first-order rate constants ($\sim 10^{-2}\ s^{-1}$) with the ferrate(VI)/(III) composite were several orders of magnitude higher than those of spontaneous hydrolysis of CWAs (10^{-8}–$10^{-6}\ s^{-1}$). The results demonstrated that the oxidative technology based on application of ferrate(VI) is very promising to decontaminate CWAs.

1. Introduction

There has been a worldwide concern to eliminate the presence of chemical warfare agents (CWAs) in the environment. Sulfur mustard (bis(2-chlorethyl) sulfide, HD), soman ((3,3′-dimethylbutan-2-yl)-methylphosphonofluoridate, GD), and *O*-ethyl *S*-[2-(diisopropylamino)ethyl] methylphosphonothiolate (VX) are examples of CWAs, which have shown extreme toxic effects through inhibition of acetylcholinesterase. CWA is also of a concern for contaminating the water supplies. Detection, decontamination, and destruction of CWAs have thus become the focus of the researchers in this field [1–3]. Generally, hydrolysis of CWAs is commonly applied for their destruction, but it has a limited use in the real-world decontamination. Natural processes are applicable; however, they are not appropriate for fast and active removal of CWAs. Conventional processes such as a phase transfer through aeration stripping and adsorption by activated charcoal usually do not give sufficient quantitative CWAs removal and decontamination. Oxidation and reduction processes have thus received attention in the past decade [4].

In the laboratory investigations, several studies have reported the degradation of CWAs using heterogeneous processes [5–7]. The studied solid surfaces include polyoxometalate (POM), vanadium oxide nanostructure, and modified titania nanotubes, which showed degradation of CWAs within hour(s). Application of advanced reduction or oxidation processes is more promising because of their fast kinetics of reactions [4,8–10]. These processes use hydrated electron (e^-_{aq}) as a reductant and hydroxyl radical ($^\bullet OH$) as an oxidant for destruction of CWAs [4]. Photolysis and photocatalytic degradation processes are relatively slow in removing CWAs [8]. Oxidation process using O_3/UV, O_3/H_2O_2, UV/H_2O_2, and $^\bullet OH$ have shown promise, but these are not efficient due to possible reaction of reactive species with constituents present in water such as O_2, HCO_3^-, and organic matter, which are present at higher concentrations compared to CWAs. There is still need for introduction of innovative reductant/oxidant agents for destruction of CWAs, which would be environmentally friendly as well as efficient in degrading CWAs. Iron based reductant (nanoscale zero-valent

* Corresponding author. Tel.: +420 585634947; fax: +420 585634958.
** Corresponding author. Tel.: +1 321 674 7310; fax: +1 321 674 8951.
E-mail addresses: zboril@prfnw.upol.cz (R. Zboril), vsharma@fit.edu (V.K. Sharma).

0304-3894/$ – see front matter © 2011 Elsevier B.V. All rights reserved.
doi:10.1016/j.jhazmat.2011.10.094

iron, nZVI) and oxidants (iron(VI), iron(IV), and their composites) are excellent alternatives, which may address concerns of currently known processes.

Nanoscale zero-valent iron particles have recently received attention due to their possible large scale application at the localities contaminated by various inorganic and organic pollutants. The nZVI particles, applicable as *in situ* reducing agent in groundwater treatment, have shown high reactivity, which caused the effective transformation of many toxic contaminants into less toxic or benign products. For example, the removal of more than seventy contaminants from water, which includes polychlorinated hydrocarbons and arsenic [11,12] was successfully accomplished by using of nZVI. Additionally, the reductive properties of elemental iron and the sorption capabilities of the subsequently formed iron oxides can also be used for removing the heavy metals by turning them into less soluble forms through changes in their oxidation state and/or by adsorption [13,14]. Iron in +6 oxidation state ($Fe^{VI}O_4^{2-}$, Fe(VI)) has also shown promise in efficient oxidation of sulfur- and nitrogen-containing compounds [15–18]. Fe(VI) has applications in oxidation of micropollutants (e.g. antibiotics), in removal of metals (e.g. arsenic) and in inactivation of microorganisms (e.g. *Escherichia coli*) [19–21]. Significantly, oxidation, coagulation, and disinfection processes can be achieved simultaneously in application of a single dose of ferrate(VI)/(III) composite, which can be prepared by thermal routes in a large-scale. Moreover, the iron(III) hydroxide nanoparticles, being the result of decomposition of $KFeO_2$ (i.e. the Fe(III) phase in composite) in reaction solutions, might act as an additional efficient sorbent.

The present paper represents the first comparative study aimed at destruction of CWAs by iron-based reduction and oxidation technologies using advantageous properties of nZVI and Fe(VI), respectively. The characterization of synthesized nZVI and ferrate(VI)/(III) composite is also presented.

2. Experimental

2.1. Syntheses of nZVI and ferrate(VI)/(III) composite

The nZVI particles were synthesized at a semi-industrial scale utilizing thermally induced solid-state reduction of hematite α-Fe_2O_3 powder (Bayferrox® 110, LANXESS, GmbH). Briefly, the iron(III) oxide powder was thermally treated (600 °C, 5 h) under hydrogen atmosphere and the nZVI particles were subsequently stabilized by controlled air-oxidation [22], which resulted in the FeO/Fe_3O_4 oxide shell on the surface of metallic particles. The weight content of Fe(0) in nZVI powder was determined to be 91%. Ferrate(VI)/(III) composite was synthesized using the optimized method of Thompson [23]. In this method, the mixture of iron(III) oxide (hematite α-Fe_2O_3 powder, Bayferrox® 110, LANXESS, GmbH) and potassium nitrate (Sigma–Aldrich Co.) in a molar ratio of 1:4 was homogenized in an agate mortar and thermally treated at 1000 °C under the stream of nitrogen gas for 30 min. The final composite obtained was composed of a mixture of Fe(VI) and Fe(III) phases, namely K_2FeO_4 and $KFeO_2$, respectively. The determined weight content of K_2FeO_4 in the composite was 31%. The synthesized ferrate(VI)/(III) composite was stored in vacuum desiccator due to the highly unstable and hygroscopic nature of both phases in the composite [24,25].

2.2. Reaction of nZVI with CWAs

The applicability of both environmentally friendly iron based materials in treatment of chemical warfare agents was tested with three representative compounds: sulfur mustard (bis(2-chlorethyl) sulfide, HD), soman ((3,3′-imethylbutan-2-yl)-methylphosphonofluoridate, GD), and *O*-ethyl *S*-[2-(diisopropylamino)ethyl] methylphosphonothiolate (VX). All CWAs were purchased from Training, Analytical and Supply Center Čereňany, Slovak Republic, and used without any further purification (purity of HD, GD and VX is 92.5%, 85.6%, and 82.9%, respectively). The nZVI specimens (1061 mg for HD, 426 mg for GD, and 553 mg for VX compound) were transferred into glass vials and 950 μl of distilled water and 50 μl of isopropyl alcohol were then added. 1 mg of CWA was added into each vial and the reaction mixtures were shaken to homogenize them. After a fixed time interval (2, 4, 8, 16, 32 and 64 min), 500 μl of the reaction mixture was withdrawn and poured into 2500 μl of *n*-hexane, followed by vigorous mixing for 1 min. The extracted CWAs were inserted into *n*-hexane and 1 ml of CWA/*n*-hexane solution was then analyzed by a gas chromatography (GC) technique to determine the content of CWA. The analogous experiments were conducted without addition of nZVI in order to evaluate the role of spontaneous hydrolysis.

2.3. Reaction of ferrate(VI)/(III) composite with CWAs

Analogously to experiments described in Section 2.2, the particular amounts of ferrate(VI)/(III) composite (505 mg for HD, 3.8 mg for GD, and 398 mg for VX compound) were dissolved in 10 ml of distilled water and 1 mg of CWA was added to this solution. The reaction mixture was vigorously shaken. After a fixed time interval (2, 4, 8, 16, 32, and 64 min), samples were extracted to vials containing 300 mg of sodium thiosulfate pentahydrate and 900 μl of nonane. The samples were then analyzed by a GC technique to determine the content of CWA.

2.4. Experimental techniques and kinetic model

Transmission ^{57}Fe Mössbauer spectra of solid samples of nZVI and ferrate(VI)/(III) composite were acquired at 300 K using a Mössbauer spectrometer at a constant acceleration mode with a ^{57}Co(Rh) source and α-Fe foil as a velocity-scale calibration standard. Scanning electron micrographs (SEM) were acquired using a field-emission scanning electron microscope SU6600 (Hitachi) operating at 5 kV and 15 kV for ferrate(VI)/(III) composite and nZVI sample, respectively. An X'Pert PRO diffractometer (PANalytical) with CoK_α radiation was employed for X-ray powder diffraction (XRD) analyses. A sample of nZVI was placed on a zero-background Si slide, gently pressed, and scanned with a step size of 0.017°. With respect to the highly hygroscopic nature of both phases in the ferrate(VI)/(III) composite, the studied sample was placed on a Pt strip and measured under vacuum in an HTK16 (Anton Paar, GmbH) high-temperature chamber at room temperature. The phase composition of the studied samples was evaluated using the X'Pert HighScorePlus software package (PANanalytical) and the PDF-4+ database (JCPDS-ICDD). Gas Chromatography 6890N (Agilent Technologies, equipped with FPD/P and FPD/S detectors and autoinjection system) was used for measurements of degradation of CWAs. For analyzing the kinetics data, an equation $c_\tau = c_0 \exp(-k_1\tau)$ was used, where c_τ denotes the residual concentration of CWA in time τ; c_0 stands for the initial concentration of CWA. The percentage of degradation (%) was calculated as $\% = [1 - (c_\tau/c_0)] \times 100$.

3. Results and discussion

3.1. Phase composition and particle size of nZVI and ferrate(VI)/(III) composite

The thermally induced solid-state processes, described in Section 2, were applied in this study due to their applicability for a large

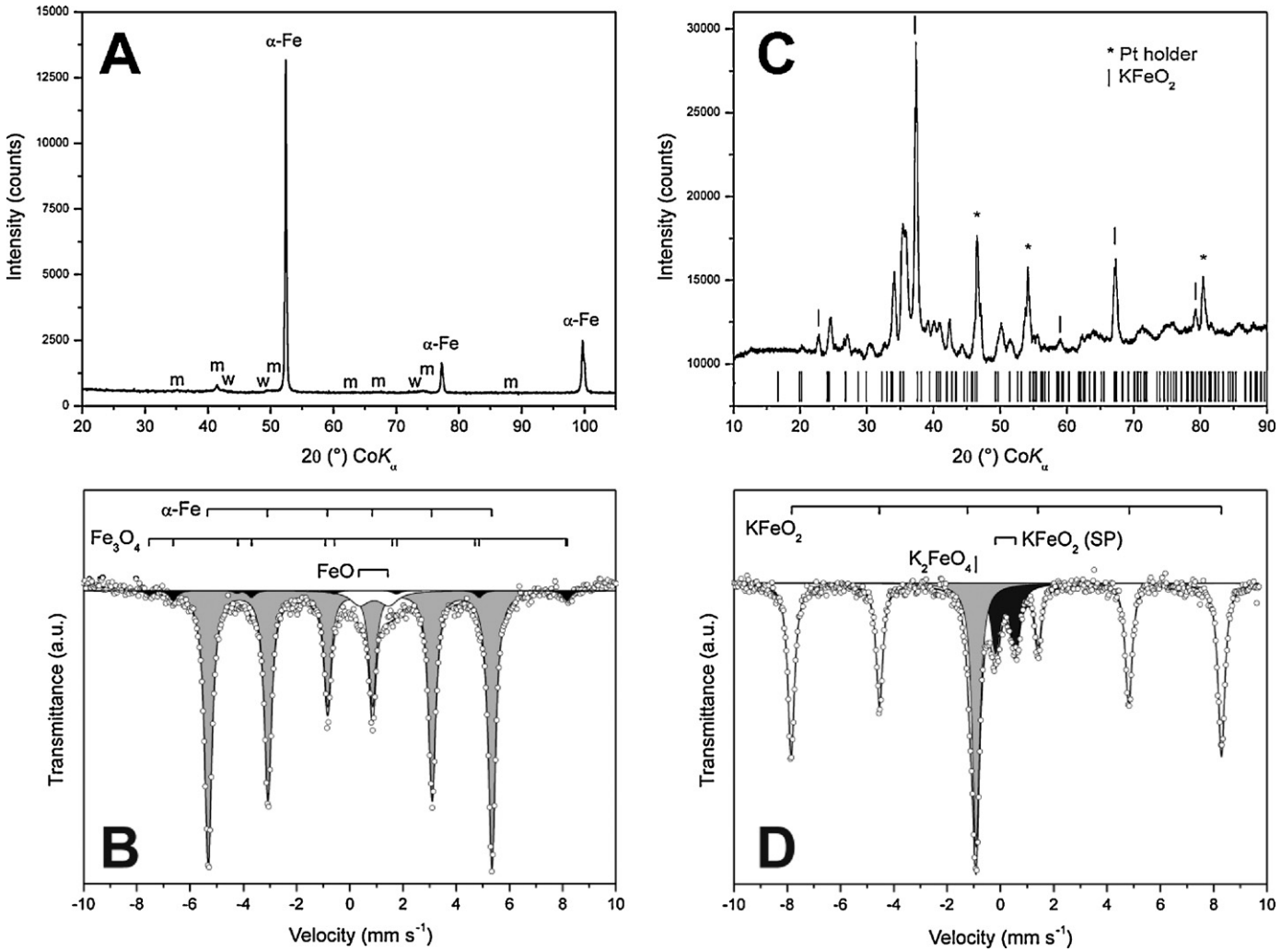

Fig. 1. X-ray powder diffraction patterns and room-temperature Mössbauer spectra of nZVI sample stabilized by Fe_3O_4/FeO oxide shell (A and B) and ferrate(VI)/(III) composite (C and D), respectively. Labels in the panel A are: α-Fe, bcc metallic iron; m, magnetite (Fe_3O_4); w, wüstite (FeO). Theoretical positions of K_2FeO_4 diffractions are shown below the experimental pattern in panel (C) (PDF 01-070-1523); SP, superparamagnetic fraction in the Mössbauer spectrum (D).

scale production of environmentally friendly reductants/oxidants. Phase composition of the samples, studied by XRD and Mössbauer spectroscopy, confirmed that the nZVI sample was composed of zero-valent iron nanoparticles (see Fig. 1) coated by a thin surface layer (4 nm thick as observed by transmission electron microscopy, not shown) of magnetite (Fe_3O_4) and wüstite (FeO). The weight content of metallic iron (91 wt%) was calculated from the relative spectral areas of the Mössbauer spectrum (see Fig. 1 and Table 1) recorded at room temperature. The particle size ranged between 30 nm and 150 nm (see SEM image in Fig. 2) with a mean diameter of 70 nm.

The sample of ferrate(VI)/(III) composite contained 31 wt% of potassium ferrate(VI), K_2FeO_4 and 69 wt% of potassium ferrite, $KFeO_2$. Weight percentages were confirmed by XRD and Mössbauer spectroscopy (see Fig. 1). However, Fe(VI)-to-Fe_{tot} atomic ratio was 0.24 according to Mössbauer spectrum analysis (see Table 1). Evidently, such synthetic procedure leads to formation of $KFeO_2$ phase both in several micrometer sized crystals and in nanometer sized particles, which were clearly evidenced as a superparamagnetic doublet fraction present in the Mössbauer spectrum (see Fig. 1) and particularly in the SEM image (see Fig. 2). The data described in the next sections are focused mainly on the comparison of reductive

Table 1
Room-temperature Mössbauer hyperfine parameters of the nZVI and Fe(VI)/Fe(III) composite samples, where δ is the isomer shift, ΔE_Q is the quadrupole splitting (shift), B_{hf} is hyperfine magnetic field (±0.3 T), and RA is the relative area (±1%).

Sample	Component	$\delta \pm 0.01$ (mm/s)	$\Delta E_Q \pm 0.01$ (mm/s)	$B_{hf} \pm 0.3$ (T)	RA ± 1 (%)
nZVI	α-Fe	0.01	0.00	33.1	91
	FeO	0.92	1.10	–	5
	Fe_3O_4 (A)	0.37	0.06	49.1	1
	Fe_3O_4 (B)	0.67	0.18	46.0	3
Ferrate(VI)/(III) composite	Fe(VI)	−0.92	–	–	24
	Fe(III)	0.18	0.08	50.2	61
	Fe(III) SP	0.19	0.74	–	15

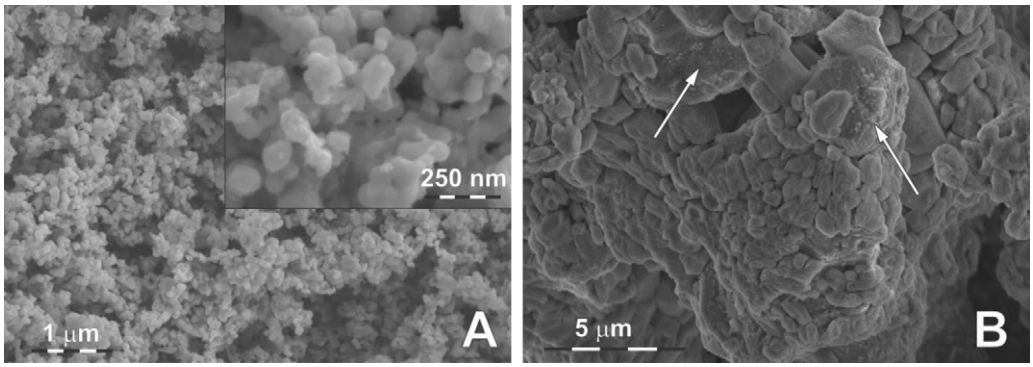

Fig. 2. SEM images of nZVI powder (A) and the ferrate(VI)/(III) composite (B). The arrows point to the areas with a high density of nanoparticles ($KFeO_2$) on the surface of micrometer sized particles.

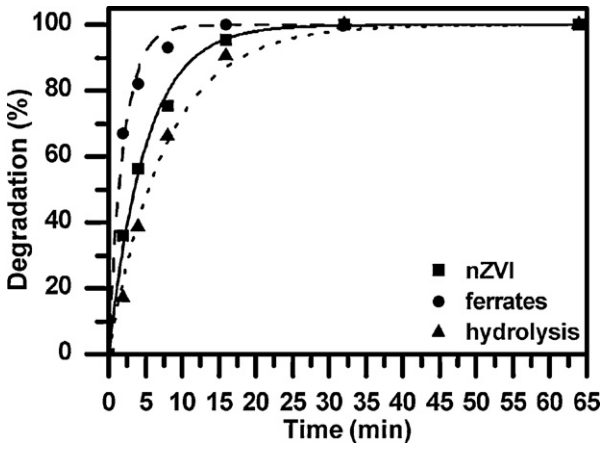

Fig. 3. Time dependence of degradation of sulfur mustard by the nZVI and ferrate(VI)/(III) composite. Data corresponding to spontaneous hydrolysis are included for comparison.

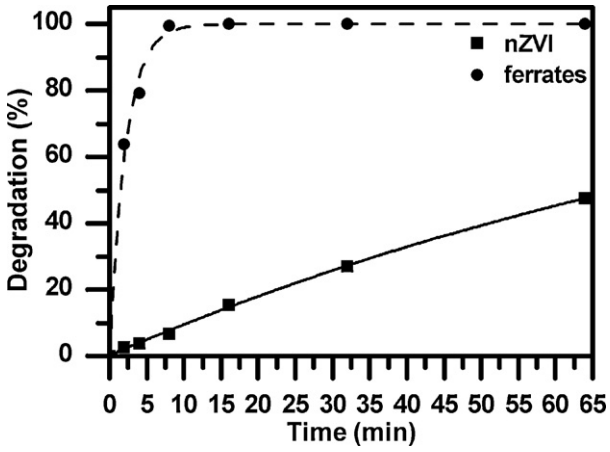

Fig. 4. Time dependence of degradation of soman by the nZVI and ferrate(VI)/(III) composite.

and oxidative environmentally friendly iron-based technologies for the treatment of CWAs. However, a role of nanodimensional nature of materials and their sorption properties should also be taken into account.

3.2. Degradation of sulfur mustard (HD) with nZVI and ferrate(VI)/(III) composite

The kinetic curves, shown in Fig. 3, represent the rate of sulfur mustard (HD) degradation by nZVI and ferrate(VI)/(III) composite. In addition to chemical degradation, hydrolysis of HD may occur simultaneously [1]; hence a separate study of this hydrolytic process was conducted and the results are shown in Fig. 3. The rate constant for spontaneous hydrolysis was found to be $2.14 \times 10^{-3}\ s^{-1}$ whereas, after the addition of nZVI, the rate constant was determined to be $3.30 \times 10^{-3}\ s^{-1}$. This implies that the spontaneous hydrolytic reaction of sulfur mustard occurred predominantly compared to the possible degradation of HD with nZVI.

In the case of ferrate(VI)/(III) composite, the rate constant of sulfur mustard degradation was $8.27 \times 10^{-3}\ s^{-1}$. As shown in Fig. 3, HD was completely decontaminated within 16 min. The rate constant for the reaction of HD with ferrate(VI)/(III) composite was approximately four times higher than its above-presented spontaneous hydrolytic degradation.

3.3. Degradation of soman (GD) with nZVI and ferrate(VI)/(III) composite

The reaction of soman in a mixture with zero-valent iron proceeded slowly ($k_1 = 1.47 \times 10^{-4}\ s^{-1}$). The nZVI showed only a limited detoxification capacity as only 40% of CWA was degraded after 60 min of the reaction (see Fig. 4). Nevertheless, the rate constant determined for degradation of soman by nZVI species was about two orders of magnitude higher than that observed for the spontaneous hydrolytic degradation (see Table 2). This suggests potentially limited exploitation of nZVI for the treatment of soman by a reductive process.

The oxidative degradation of soman using ferrate(VI)/(III) composite turned out to be fast as the complete degradation was reached within 8 min. Compared to the spontaneous hydrolysis of soman (see Table 2), the obtained rate constant ($k_1 = 7.66 \times 10^{-3}\ s^{-1}$) was three orders of magnitude higher (see Table 2). The results support the potential exploitation of ferrate(VI) for a rapid oxidative degradation of soman.

Table 2
The rate constants obtained for degradation of CWAs by nZVI and ferrate(VI)/(III) composite where HD is sulfur mustard (bis(2-chlorethyl) sulfide), GD is soman ((3,3′-imethylbutan-2-yl)-methylphosphonofluoridate), and VX is *O*-ethyl *S*-[2-(diisopropylamino)ethyl] methylphosphonothiolate. For comparison, the rate constants corresponding to spontaneous hydrolysis are also listed.

CWA	Spontaneous hydrolysis k_1 (s^{-1})	nZVI k_1 (s^{-1})	Ferrate(VI)/(III) composite k_1 (s^{-1})
HD	2.14×10^{-3}	3.30×10^{-3}	8.27×10^{-3}
GD	3.70×10^{-6}	1.47×10^{-4}	7.66×10^{-3}
VX	1.00×10^{-8}	7.16×10^{-5}	1.17×10^{-2}

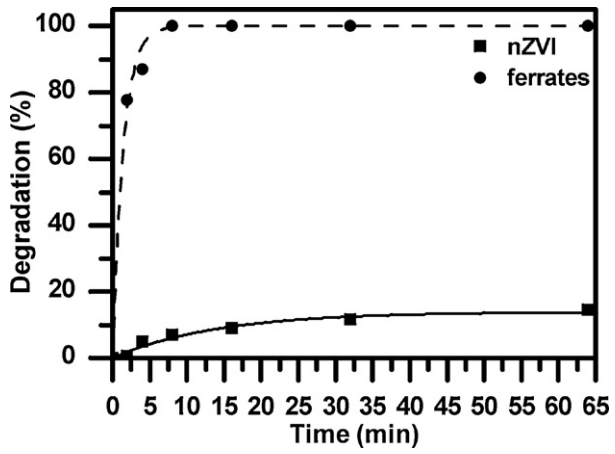

Fig. 5. Time dependence of degradation of VX compound by the nZVI and ferrate(VI)/(III) composite.

3.4. Degradation of the VX compound with nZVI and ferrate(VI)/(III) composite

Fig. 5 shows comparison of degradability of the VX compound through the reductive and oxidative processes by applying nZVI and ferrate(VI)/(III) composite, respectively. After 1 h of treatment of VX compound by nZVI, we obtained only ~20% decrease (see Fig. 5). The degradation of VX by nZVI was considerably lower compared to soman detoxification. Furthermore, the obtained rate constant ($7.16 \times 10^{-5}\,s^{-1}$) was higher compared to that obtained for the spontaneous hydrolytic degradation (see Table 2).

The oxidative degradation of VX with ferrate(VI)/(III) composite was efficient (see Fig. 5) and complete removal was achieved in ~10 min. The estimated rate constant ($1.17 \times 10^{-2}\,s^{-1}$) was approximately eight orders of magnitude higher than that obtained by the spontaneous hydrolysis (see Table 2).

4. Conclusions

The Mössbauer spectroscopy and scanning electron microscopy established oxidation states of iron and nanocrystalline character, respectively, of thermally synthesized iron-based species including composites designed for CWAs degradation. The in-detail monitored process of CWAs degradation using synthesized nZVI and ferrate(VI)/(III) composite showed that the oxidation promoted by the ferrate(VI)/(III) composite was more effective in removing CWAs than the reduction by zero-valent iron. Both nZVI and ferrate(VI)/(III) composite removed HD completely; however, spontaneous hydrolysis of HD played a significant role during its degradation by either reduction or oxidation process. Reactions of GD and VX with Fe(VI) were rapid with complete degradations achieved within 10 min. On the contrary, the efficiency of GD and VX degradation by nZVI was found to be below 50% upon reaction time of ~1 h. Future studies may include investigation of causes of such low capacity of nZVI to reduce CWAs. Future work includes the detailed characterization of degradation products, which would help understand the mechanism by which Fe(VI) oxidizes CWAs and support benign character of CWAs degradation processes using iron-based reductants and oxidants.

Acknowledgements

This work has been supported by the grants from the Ministry of Education of the Czech Republic (projects no. 1M6198959201 and MSM6198959218), grant from the Academy of Sciences of the Czech Republic (project no. KAN115600801) and by the Operational Program Research and Development for Innovations–European Regional Development Fund (project no. CZ.1.05/2.1.00/03.0058 of the Ministry of Education, Youth and Sports of the Czech Republic). The partial support of NATO Collaborative Linkage Grant (grant no. CBP.EAP.CLG.983119) is also acknowledged. We thank Dalibor Jančík and Klára Šafářová for microscopic characterization of solid samples. Authors also thank reviewers for their comments which improved the paper greatly.

References

[1] Y.C. Yang, J.A. Baker, J.R. Ward, Decontamination of chemical warfare agents, Chem. Rev. 92 (1992) 1729–1743.
[2] Y. Yang, H.F. Ji, T. Thundat, Nerve agents detection using a Cu^{2+}/L-cysteine bilayer-coated microcantilever, J. Am. Chem. Soc. 125 (2003) 1124–1125.
[3] G.W. Wagner, Y.C. Yang, Rapid nucleophilic/oxidative decontamination of chemical warfare agents, Ind. Eng. Chem. Res. 41 (2002) 1925–1928.
[4] A. Abbott, T. Sierakowski, J.J. Kiddle, K.K. Clark, S.P. Mezyk, Detailed investigation of the radical-induced destruction of chemical warfare agent simulants in aqueous solution, J. Phys. Chem. C 114 (2010) 7681–7685.
[5] B. Singh, T.H. Mahato, A.K. Srivastava, G.K. Prasad, K. Ganesan, R. Vijayaraghavan, R. Jain, Significance of porous structure on degradation of 2 2′-dichloro diethyl sulphide and 2-chloroethyl ethyl sulphide on the surface of vanadium oxide nanostructure, J. Hazard. Mater. 190 (1–3) (2011) 1053–1057.
[6] A. Sharma, A. Saxena, B. Singh, In-situ degradation of sulphur mustard using (1R)-(−)-(camphorylsulphonyl) oxaziridine impregnated adsorbents, J. Hazard. Mater. 172 (2009) 650–653.
[7] K.G. Prasad, B. Singh, K. Ganesan, A. Batra, T. Kumeria, P.K. Gutch, R. Vijayaraghavan, Modified titania nanotubes for decontamination of sulphur mustard, J. Hazard. Mater. 167 (2009) 1192–1197.
[8] S. Neatu, V.I. Parvulescu, G. Epure, E. Preda, V. Somoghi, A. Damin, S. Bordiga, A. Zecchina, Photo-degradation of yperite over V, Fe and Mn-doped titania-silica photocatalysts, Phys. Chem. Chem. Phys. 10 (2008) 6562–6570.
[9] D.A. Panayotov, J.R. Morris, Catalytic degradation of a chemical warfare agent simulant: Reaction mechanisms on TiO_2-supported Au nanoparticles, J. Phys. Chem. C 112 (2008) 7496–7502.
[10] B. Veriansyah, J.D. Kim, J.C. Lee, Destruction of chemical agent simulants in a supercritical water oxidation bench-scale reactor, J. Hazard. Mater. 147 (2007) 8–14.
[11] W. Zhang, Nanoscale iron particles for environmental remediation: an overview, J. Nanopart. Res. 5 (2003) 323–332.
[12] P.G. Tratnyek, R.L. Johnson, Nanotechnologies for environmental cleanup, Nano Today 1 (2006) 44–48.
[13] B. Geng, Z.H. Jin, T.L. Li, X.H. Qi, Kinetics of hexavalent chromium removal from water by chitosan-Fe^0 nanoparticles, Chemosphere 75 (2009) 825–830.
[14] S. Klimkova, M. Cernik, L. Lacinova, J. Filip, D. Jancik, R. Zboril, Zero-valent iron nanoparticles in treatment of acid mine water from in situ uranium leaching, Chemosphere 82 (2011) 1178–1184.
[15] V.K. Sharma, Oxidation of inorganic compounds by ferrate(VI) and ferrate(V): one-electron and two-electron transfer steps, Environ. Sci. Technol. 44 (2010) 5148–5152.
[16] V.K. Sharma, Oxidation of nitrogen-containing pollutants by novel ferrate(VI) technology: a review, J. Environ. Sci. Health A: Tox. Hazard. Subst. Environ. Eng. 45 (2010) 645–667.
[17] V.K. Sharma, Oxidation of inorganic contaminants by ferrates (VI, V, and IV)-kinetics and mechanisms: a review, J. Environ. Manage. 92 (2011) 1051–1073.
[18] V.K. Sharma, G.W. Luther, F.J. Millero, Mechanisms of oxidation of organosulfur compounds by ferrate(VI), Chemosphere 82 (2011) 1083–1089.
[19] V.K. Sharma, X.Z. Li, N. Graham, R.A. Doong, Ferrate(VI) oxidation of endocrine disruptors and antimicrobials in water, J. Water Supply: Res. Technol.–AQUA 57 (2008) 419–426.
[20] A. Jain, V.K. Sharma, O.S. Mbuya, Removal of arsenite by Fe(VI), Fe(VI)/Fe(III), and Fe(VI)/Al(III) salts: effect of pH and anions, J. Hazard. Mater. 169 (2009) 339–344.
[21] V.K. Sharma, F. Kazama, H. Jiangyong, A.K. Ray, Ferrates (iron(VI) and iron(V)): environmentally friendly oxidants and disinfectants, J. Water Health 3 (2005) 45–58.
[22] J. Filip, R. Zboril, O. Schneeweiss, J. Zeman, M. Cernik, P. Kvapil, M. Otyepka, Environmental applications of chemically pure natural ferrihydrite, Environ. Sci. Technol. 41 (2007) 4367–4374.
[23] J.A. Thompson, Process for producing alkali metal ferrates. U.S. Patent No. 4385045.
[24] L. Machala, R. Zboril, V.K. Sharma, J. Filip, O. Schneeweiss, Z. Homonnay, Mössbauer characterization and in situ monitoring of thermal decomposition of potassium ferrate(VI), K_2FeO_4 in static air conditions, J. Phys. Chem. B 111 (2007) 4280–4286.
[25] L. Machala, R. Zboril, V.K. Sharma, J. Filip, D. Jancik, Z. Homonnay, Transformation of solid potassium ferrate(VI) (K_2FeO_4): mechanism and kinetic effect of air humidity, Eur. J. Inorg. Chem. 8 (2009) 1060–1067.